THE JOURNAL OF BIOLOGICAL CHEMISTRY Vol. 277, No. 33, Issue of August 16, pp. 30091–30101, 2002
Printed in U.S.A.

Slug Is a Novel Downstream Target of MyoD

TEMPORAL PROFILING IN MUSCLE REGENERATION*

Received for publication, March 19, 2002, and in revised form, May 15, 2002
Published, JBC Papers in Press, May 21, 2002, DOI 10.1074/jbc.M202668200

Po Zhao‡, Simona Iezzi§, Ethan Carver¶, Devin Dressman‡, Thomas Gridley¶, Vittorio Sartorelli§, and Eric P. Hoffman‡‖

From the ‡Research Center for Genetic Medicine, Children's National Medical Center, and Genetics Program, George Washington University, Washington, D. C. 20010, the §Muscle Gene Expression Group, Laboratory of Muscle Biology, NIAMS, National Institutes of Health, Bethesda, Maryland 20892, and ¶The Jackson Laboratory, Bar Harbor, Maine 04609

Temporal expression profiling was utilized to define transcriptional regulatory pathways *in vivo* in a mouse muscle regeneration model. Potential downstream targets of MyoD were identified by temporal expression, promoter data base mining, and gel shift assays; *Slug* and *calpain 6* were identified as novel MyoD targets. *Slug*, a member of the snail/slug family of zinc finger transcriptional repressors critical for mesoderm/ectoderm development, was further shown to be a downstream target by using promoter/reporter constructs and demonstration of defective muscle regeneration in *Slug* null mice.

The molecular basis for development of muscle has been a popular model for the study of cell fate and differentiation. Two experimental systems have been used extensively: vertebrate (chick, zebrafish, and mouse) embryos have been used to define the signals involved in patterning and commitment of cells during embryonic muscle development (1–3), and cultured cells have been used to define key transcriptional pathways. Particularly important has been the identification of four basic helix-loop-helix transcription factors (myogenic regulatory factors (MRFs))[1] that were able to force non-myogenic cells into a myogenic lineage *in vitro* (MyoD, myf5, myogenin, and MRF4) (4–7). Studies have included definition of binding partners, binding site sequences (E-boxes), downstream target promoters, modulation by acetylation, and timing of expression during development and differentiation, both *in vivo* and *in vitro* (8).

The most extensively studied MRF is MyoD. MyoD binding sites have been defined in a series of downstream target muscle genes, where either single binding sites of variable affinity or multiple cooperative binding sites have been defined (9–12). MyoD forms hetero- or homodimers with E proteins and has been shown to bind specific sequences known as E-boxes ($CA_{nn}TG$) (13). E-boxes have been found in the promoters of many skeletal muscle-specific genes, and they mediate gene activation in the presence of MyoD (14). More recent studies have begun to define chromatin remodeling induced by MyoD binding (requiring SWI/SNF complexes) (15), and the critical role of acetylation of the MyoD protein in transcriptional activation mediated by p300/CBP-associated factor and p300 acetyltransferases and histone deacetylase 1 (16–22). In addition, MyoD transcriptional complexes can be modulated by MAPK signaling, specifically MEK1, although this does not involve direct phosphorylation of MyoD (23).

Although cultured cell transfection experiments have suggested binding site selection for MyoD and the other MRFs based on differential activation of downstream targets during overexpression of these factors, these have not led to the definition of discriminatory sequences that dictate specific MRF protein binding at specific target genes during myogenic development (24, 25). Indeed, it has also become clear that both the transcription factors and DNA target sequences are promiscuous, with MyoD, myf-5, and myogenin all capable of binding the same downstream target promoter in differentiating cultured myogenic cells by chromatin immunoprecipitation assays (25). Likewise, recent dominant-negative fusion construct studies have shown that the protein binding partner selection of MyoD and myogenin *in vitro* may not reflect binding preference *in vivo*, despite co-expression of the factors in the myogenic cells under study (26).

Murine knock-outs of the MRF genes have provided an additional perspective in defining the roles of *MyoD* and others. *MyoD* knock-outs show relatively little overt phenotype, which has been interpreted as being indicative of functional redundancy of the MRFs (27). However, *MyoD*−/− animals show defective myogenic differentiation in culture and slowed regeneration of skeletal muscle *in* vivo (28–32). The phenotype of *MyoD* knock-out muscle and cultured cells has been difficult to integrate with the DNA/protein interaction data into a specific molecular genetic pathway, perhaps because *MyoD* may have different roles in embryonic development, muscle maturation, and differentiation in cultured cells.

The specific hierarchy of MRFs and co-regulatory proteins (sonic hedgehog family, MEFs, E proteins, and others) has been similarly difficult to dissect in studies of embryogenesis. Although *MyoD* clearly seems to be regulated by sonic hedgehog, Wnt factors, and other signals, it is not known how *MyoD* transcription is initiated and maintained by these signals (33).

* This work was supported by the Muscular Dystrophy Association (to E. P. H.) and by Grants 1-UO1-HL66614 (to E. P. H.), HOPGENE, and NIH-RO1-HD34883 (to T. G.) from the Programs in Genomic Applications, NHLBI, National Institutes of Health. The costs of publication of this article were defrayed in part by the payment of page charges. This article must therefore be hereby marked "*advertisement*" in accordance with 18 U.S.C. Section 1734 solely to indicate this fact.

‖ To whom correspondence should be addressed: Research Center for Genetic Medicine, Children's National Medical Center, 111 Michigan Ave. NW, Washington. D. C. 20010. Tel.: 202-884-6011; Fax: 202-884-6014; E-mail: ehoffman@cnmcresearch.org.

[1] The abbreviations used are: MRFs, myogenic regulatory factors; bHLH, basic helix-loop-helix; IGF1, insulin-like growth factor 1; sFRP4, secreted frizzled-related protein 4; Peg3, paternally expressed gene *3*, TM4SF6, transmembrane 4 superfamily member 6; MCK, muscle creatine kinase; ChIP, chromatin immunoprecipitation; GM, growth medium; DM, differentiation medium; CTX, cardiotoxin; RT-PCR, reversed transcription PCR; QMF-PCR, quantitative multiplex fluorescence PCR; avg diff, average difference; CMV, cytomegalovirus; DMEM, Dulbecco's modified Eagle's medium; MAPK, mitogen-activated protein kinase; MEK1, MAPK/extracellular signal-regulated kinase kinase 1.

For example, in zebrafish knock-outs for *sonic hedgehog*, *MyoD*, and *myf5* seem to be appropriately expressed initially, but then maintenance of expression is sustained in some regions but not others (3).

Muscle tissue, and the constituent terminally differentiated muscle fibers, are able to regenerate after damage. The regeneration process is known to re-capitulate many of the features of myogenic development, with activation of myogenic stem cells (satellite cells), proliferation, differentiation, and fusion of these cells into myotubes, and then maturation into the large syncytial myofibers. Studies of MRFs during muscle regeneration *in vivo* have shown clear temporal patterns of expression, which correlate with the differentiation state of the cells in the regenerating muscle (34, 35). Thus, staged regeneration of muscle serves as a model for cell commitment, differentiation, and maturation.

We sought to dissect the likely highly complex cascade of transcription factors and downstream targets using a more global, non-"candidate gene" approach. Dissection of novel transcriptional pathways has been accomplished in yeast by staging yeast cultures, exposing the cultures to a specific stimulus, and then conducting temporal expression profiling (microarrays) to define coordinately regulated genes (36, 37). However, such studies have not yet been reported in higher organisms, presumably due to the difficulty in staging mammalian cells *in vivo*, and the greater cellular and molecular complexity of experimental systems. Importantly, the sensitivity of human expression profiling resources is quickly approaching that of yeast, with a two-chip set containing every transcription unit in the human genome to be released shortly.[2] Increasingly accurate bioinformatic-driven probe design and synthesis, the correlation of expressed sequence tag databases with genomic data, and the use of a high level of redundancy in testing of each transcript unit serve to make emerging oligonucleotide-based GeneChips quite sensitive and specific tools.

We hypothesized that staged induction of muscle degeneration in murine muscle and expression profiling of specific time points during regeneration would allow us to define coordinately expressed genes and, thereby, define novel downstream targets of MyoD. Here, we report the successful identification of novel downstream targets of MyoD using this global genomics approach and show that one of the novel downstream targets, *Slug*, is necessary for appropriate muscle regeneration. These data also provide the first intersection between two important transcriptional pathways, namely the bHLH MRF pathway, and the *snail*/*Slug* developmental pathway. The publicly available transcription profiles can be used to define the temporal clusters for any transcription factor and downstream target and should greatly assist in the definition of the *in vivo* gene pathways for a popular experimental system for studying molecular development.

EXPERIMENTAL PROCEDURES

Induction of Staged Muscle Degeneration/Regeneration—Staged skeletal muscle degeneration/regeneration was induced by injection of cardiotoxin into mouse gastrocnemius muscle. Injection was done by using a custom injection manifold, Microlab 500 series (Hamilton), which has 10 needles in a 1-cm^2 area. Two-month-old C57BL10 mice (JAX mice, Bar Harbor, ME) were anesthetized by intraperitoneal injection of xylazine (7 mg/kg body weight) and ketamine HCl (70 mg/kg body weight). Each muscle was injected with 100 μl of 10 mM cardiotoxin (Calbiochem). Both contralateral gastrocnemius muscles were injected. Two mice were injected and then sacrificed at each of the following time points: time 0 (no injection), 12 h, day 1, day 2, day 4, and day 10. Gastrocnemius muscles were carefully dissected at tendon insertion points and flash-frozen in isopentane cooled in liquid nitrogen. Thus, four muscles were harvested at each time point.

Each muscle was examined histologically in the belly (center) of the muscle. Cryosections (8 μm) were cut using an IEC Minotome cryostat, collected on Superfrost Plus slides (Fisher Scientific), and stained with hematoxylin and eosin. At each time point, two of the four muscles showing the most extensive and consistent histological changes were used for expression profiling on individual GeneChips.

Expression Profiling—Selected gastrocnemius muscles were homogenized in guanidinium thiocyanate homogenization buffer (4.0 M guanidinium thiocyanate, 0.1 M Tris-Cl, pH 7.5, 1% β-mercaptoethanol) using a Polytron homogenizer (Brinkmann Instruments). Total RNA was extracted by centrifuging the homogenate at 25,000 rpm for 24 h in a CsCl cushion (5.7 M CsCl, 0.01 M EDTA, pH 7.5). Double-stranded cDNA was synthesized from 8 μg of total RNA using SuperScript Choice system (Invitrogen) and T7-(dT_{24}) primer (Geneset Corp). cDNA was purified using a Phase Lock Gel (Eppendorf-5 Prime). Biotin-labeled cRNA was then synthesized from double-stranded cDNA by *in vitro* transcription using a BioArray HighYield RNA transcript labeling kit (Affymetrix). cRNA was purified using an RNeasy Mini kit (Qiagen), fragmented, and hybridized to Murine Genome U74A version 1 chips for 16 h. GeneChips were then washed and stained on the Affymetrix Fluidics Station 400 following protocols of Affymetrix. Staining images were read using the Hewlett-Packard G2500A Gene Array Scanner and stored in an Affymetrix Microarray Laboratory Information Management System.

Gene lists with -fold changes at each time point are available on our web site (microarray.cnmcresearch.org, Programs in Genomic Applications). More detailed descriptions of methods for generating gene lists are also on the website (microarray.cnmcresearch.org/programs in genomic application). All image files (.dat) and absolute analysis files (.chip) corresponding to each expression profile are also available on our website.

Data Analysis—Primary data analysis was done using Affymetrix Microarray Suite 4.0. This includes absolute analysis and comparison analysis. Absolute analysis calculates the intensity of the hybridization signals from a single array and determines whether a transcript is present or absent in the sample based on hybridization of 16–20 perfect match and mismatch probe pairs for each gene under study. Comparison analysis compares signals from two probe arrays and assigns a difference call to each transcript that indicates expression changes. In comparison analysis, time 0 arrays were used as the baseline. At each time point, four pair-wised comparison analysis results were done as we have previously described (38). Comparison analysis results were further processed to select genes with >2-fold changes and to provide an average -fold change using a Microsoft Excel spreadsheet.

Absolute analysis results derived from Microarray Suite 4.0 were used for temporal clustering as follows. First, an SAS program was written and used to exclude the probe sets that showed absent calls in all 12 expression profiles. Then, the average difference (absolute analyses) of the surviving probe sets was loaded into GeneSpring for all 12 profiles. A hierarchical clustering algorithm was used to temporally group those probe sets based on their expression pattern across the six time points. Gene lists nucleated with a single gene were generated by using a 0.95 or 0.97 standard correlation coefficient to the expression of the nucleating gene.

Quantitative Multiplex Fluorescence PCR—Five μg of total RNA was used to synthesize cDNA using oligo(dT) primer (Invitrogen) in a 20-μl reaction. One μl of cDNA was then used for RT-PCR. Primers used for RT-PCR are *Slug* (U79550) forward: 5′-gcagtaatacaatgcccctcc-3′, *Slug* reverse: 5′-ggcgtggctattaaccgtacc-3′; NIPI-like protein (U67328) forward: 5′-aacagggaacctatggtggc-3′, reverse: 5′-ctgtccacagggtgactgaag-3′; CMP-*N*-acetylneuraminic acid synthetase (AJ006215) forward: 5′-gacctagtcttgctccgacctc-3′, reverse: 5′-cagggtgtcttaccagactc-3′. Forward primers were labeled with an infrared fluorescent dye (IRDye 700, LI-COR). PCR were done at 94 °C for 30 s, 55 °C for 30 s, and 72 °C for 30 s for 15 cycles, and then a 72 °C extension for 7 min. Multiplex RT-PCR products were run and quantitated on a 5.5% gel using a LI-COR DNA analyzer. PCR products were 135 bp (*Slug*), 142 bp (NIPI-like protein), and 128 bp (CMP-*N*-acetylneuraminic acid synthetase). PCR products were quantitated using Gene ImagIR 3.56 (LI-COR). Expression of *Slug* was normalized to that of NIPI-like protein (control1) and CMP-*N*-acetylneuraminic acid synthetase (control2) by using the formula, (*Slug*/control1 + *Slug*/control2)/2.

Gel Shift Assay—21- or 22-bp double-stranded oligonucleotide probes selected from putative promoter regions of mouse and human *Slug*, human *calpain 6*, *IGF-1*, *Peg3*, *sFRP4*, and *TM4SF6* genes were used for MyoD gel shift assay. A 21-bp MyoD binding probe from muscle

[2] Affymetrix, personal communication.

creatine kinase (*MCK*) promoter (Geneka Biotech) was used as a control. The oligonucleotide probes were labeled with [γ-^{32}P]ATP and purified with MicroSpin G-25 columns (Amersham Biosciences). The gel shift assay was done using a MyoD gel shift kit (Geneka Biotech). Nuclear extracts (10 μg) from C2C12 cells were incubated with binding buffer for 20 min at 4 °C and then incubated with 5 ng of labeled oligonucleotide probes for an additional 20 min at 4 °C. For the competition test, 100 times more of unlabeled wild-type or mutant *MCK* probes (500 ng) were added to each reaction. For the supershift assay, 1 μl of antibodies against MyoD (M318X, Santa Cruz Biotechnology) or rabbit IgG (Santa Cruz Biotechnology) were incubated with nuclear extract mix for 20 min before adding labeled oligonucleotide probes. The reaction mixture was subjected to 10% polyacrylamide gel electrophoresis at 90 V for 2.5 h. Gels were dried and exposed to x-ray film.

Chromatin Immunoprecipitation Assay—Murine myoblast (C2C12) were cultured in 10-cm plates in 20% fetal bovine serum until 75% confluent. Then serum was withdrawn, and the cells were allowed to differentiate for 2 days. MyoD-negative murine fibroblasts (NIH 3T3) were cultured until 100% confluent. The cells were fixed with 1% of formaldehyde to cross-link protein and DNA then harvested, and chromatin was extracted. Chromatin was sonicated to about 600-bp fragments. Chromatin fragments were pre-cleared with protein A-agarose (Invitrogen) and then incubated with anti-MyoD antibody (M318X, Santa Cruz Biotechnology) or rabbit IgG and rotated overnight at 4 °C. Chromatin bound by antibody was then precipitated with protein A-agarose, washed as described in Boyd *et al.* (39), and eluted with 50 mM $NaHCO_3$ and 1% SDS. Protein and DNA cross-linking was reversed by incubating at 67 °C in 0.3 M NaCl for 5 h. DNA was then ethanol-precipitated, digested with proteinase K, and extracted with phenol/chloroform.

A 240-bp sequence in mouse Slug promoter region (AF079305) was amplified by PCR (primers: 5′-tgccatgagcagcccattttg-3′ and 5′-ataacatcgcggtggctcagg-3′; conditions: 94 °C for 30 s, 55 °C for 30 s, and 72 °C for 30 s for 25 cycles, then an extension at 72 °C for 10 min). This fragment contains the E-box tested for the gel shift assay.

PCR Amplification of the Slug Promoter, Subcloning, and Mutagenesis—Genomic DNA was isolated from C2C12 skeletal muscle cells and mildly sheared with an 18-gauge syringe needle before PCR-mediated amplification of a 240-bp *Slug* genomic region (see "Chromatin Immunoprecipitation Assay" for primers and PCR conditions). An *Xho*I site was added to the "sense" primer, and a *Hin*dIII site was added to the "antisense" primers. After PCR amplification, the *Slug* genomic products were digested with *Xho*I and *Hin*dIII. The *Slug*-restricted fragments were subcloned in the pGL2 luciferase reporter vectors pGL2 Basic, pGL2-Promoter, and pGL2-Enhancer (Promega) digested with *Xho*I and *Hin*dIII. Two single-point mutations were introduced in the E-box (CAGCTG to AAGCTC) of the Slug promoter using the QuikChange kit (Stratagene). The mutations were confirmed by DNA sequencing of the Slug constructs.

Cells, Transfections, and Luciferase Assay—C2C12 skeletal muscle cells were cultured in growth medium (GM, DMEM supplemented with 20% fetal bovine serum). To induce differentiation, cells were switched to differentiation medium (DM, DMEM supplemented with 2% horse serum and 1× insulin, transferrin, and selenium). C3H10T1/2 mouse fibroblasts were cultured in DMEM supplemented with 10% fetal bovine serum. The CMV-MyoD expression vector has been described in Sartorelli *et al.* (16). Transfections were performed with FuGENE 6 transfection reagent (Roche Molecular Biochemicals), and luciferase activity was assayed with a Dual Luciferase Reporter Assay kit (Promega) on a microtiter luminescence detection system (MLX, Dynex). Luciferase assays were done in triplicate points and repeated twice.

Temporal expression profiling of C2C12 cell differentiation was done at 0, 4, 12, 24, and 48 h after cells were switched into differentiation medium. Two plates were done at each time point. Total RNA was isolated using TRIzol (Invitrogen). Expression profiling was done using Affymetrix GeneChips as described above.

RESULTS

Induction of Staged Muscle Degeneration/Regeneration—Staged skeletal muscle degeneration/regeneration was induced by intramuscular injection of cardiotoxin (CTX) using a custom injection manifold (10 needles in 1 cm^2). Twelve mice were injected in both gastrocnemii, and four muscles were collected at each of six time points following CTX injection (0, 12 h, 1 day, 2 days, 4 days, and 10 days). Cryosections from the center (belly) of each muscle were histologically examined and showed

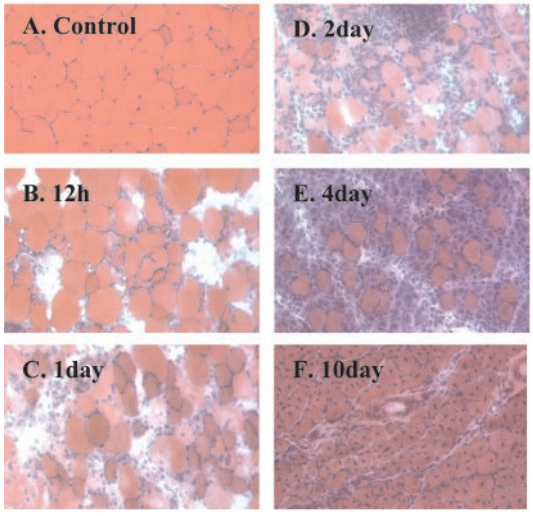

FIG. 1. **Staged muscle degeneration/regeneration induced by cardiotoxin (CTX).** Shown is hematoxylin and eosin staining of mouse gastrocnemius muscle at time 0 (*A*), 12 h (*B*), day 1 (*C*), day 2 (*D*), day 4 (*E*), and day 10 (*F*) after cardiotoxin injection. Progressive inflammation was seen from 12 h to day 2. Regenerating muscle fibers appeared at day 4. Approximately half of the muscle fibers showed evidence of regeneration at day 10 (central nuclei).

the expected, staged features of myofiber degeneration and regeneration (Fig. 1). Two of the four muscles from each time point were selected for expression profiling, based upon the observation of the most consistent histopathology throughout the muscle for that time point. Because some replicates were from the same animal, and some were from different animals, it was possible that the coefficient of variance was greater between inbred mice, compared with that within the same mouse, and this could skew our data interpretation. We therefore analyzed a large series of expression profiles by correlation coefficients to determine if inter-animal variability was greater than intra-animal variability for any specific time point following regeneration. We examined a large (27 time points, 54 GeneChip profiles) muscle regeneration expression profiling dataset[3] with duplicates of each time point derived from muscles of the same animal (18 time points) or different animals (9 time points). Correlation coefficients (R) of the two replicate profiles at each time point were calculated. The average of the R values of the expression profiles for replicates from the same animal ($r = 0.97 \pm 0.03$ ($\pm$S.D.)) was identical to that for replicates from different animals ($r = 0.97 \pm 0.03$). Student's t test showed that R values from the two groups were not different ($p = 0.96$). This suggests that inbred mice are highly similar to each other and that that variation between individual inbred mice is not a significant source of variability of expression profiling data.

Expression Profiling of Muscle Degeneration/Regeneration—The two gastrocnemii for each time point were independently solubilized, RNA was purified, and biotinylated cRNA was produced. Biotinylated cRNA samples (10 μg) were hybridized individually to U74A version 1 murine oligonucleotide arrays. Quality control measures included >4-fold cRNA amplification (from total RNA/cDNA), scaling factors <2 to reach a whole-chip normalization of 800, and visual observation of hybridization patterns for chip defects (see microarray.cnmcresearch.org for further descriptions). A data mask was used to filter out incorrect probe sets on the version 1 U74A chip, and the remaining 10,000 genes were used for data analysis.

Data was analyzed by two methods. First, Affymetrix soft-

[3] P. Zhao and E. P. Hoffman, unpublished data.

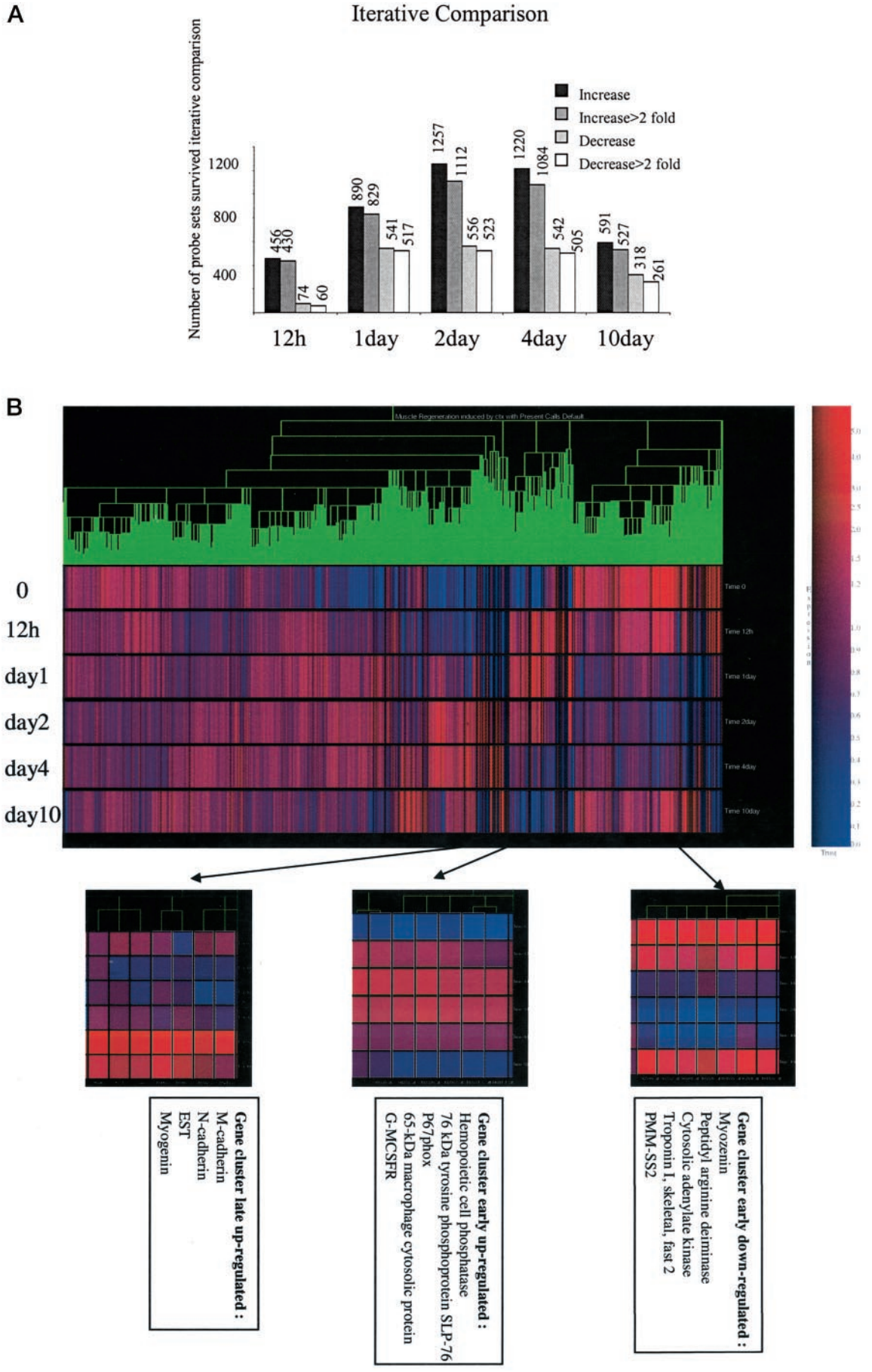

FIG. 2. **Iterative comparison and hierarchical clustering.** *A*, muscle degeneration/regeneration involves a large number of differentially expressed genes. Shown is the number of genes significantly up-regulated, up-regulated more than 2-fold, down-regulated, and down-regulated

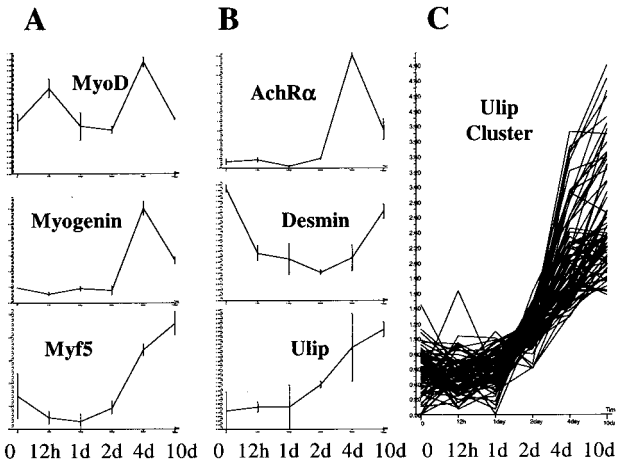

FIG. 3. **Regulation of myogenic regulatory factors and temporal clustering of downstream target genes identifies putative genes regulated by MyoD.** *A*, shown are the expression curves of transcriptional factors *Myf5*, *MyoD*, and *Myogenin*, over the six degeneration/regeneration time points with standard errors corresponding to duplicate profiles. *MyoD* transcription was up-regulated 1.8-fold at 12 h and 2.2-fold at day 4 post-injection. *Myogenin* transcription was up-regulated 8-fold at day 4 and 3.4-fold at day 10 post-injection. Day 4 is an active muscle regenerating time point. *B*, temporal profiles of genes known to be directly regulated by MyoD (*AChRα*, *desmin*, and *Ulip*). *C*, *Ulip* was used to nucleate a temporal cluster of candidate genes for MyoD regulation. The genes in this cluster were further used to identify potential MyoD downstream genes by data mining for putative E-box sequences in the gene promoters of the cluster members.

ware was used to interpret the hybridization patterns across the 20 probe pairs (40 oligonucleotides) for each gene and each profile independently, with default assignment of present/absent calls, and avg diff hybridization intensity values (.cel files). We then used our previously reported iterative comparison survival method (38), where each pair of profiles per time point (derived from independent muscle samples) was compared with the time 0 profiles, with four resulting comparison analyses. Those genes showing a >2-fold expression change by Affymetrix Microarray Suite 4.0 in each of the four possible comparisons were then retained as "significantly changed" expression. We have shown this method to be a highly specific and stringent, but relatively insensitive analytical method (40). The total number of up-regulated and down-regulated genes using this method showed a gradual increase until day 4, whereupon expression changes decreased at day 10 (Fig. 2*A*). Most of the genes up-regulated at 12 h were associated with inflammation and immune responses, consistent with the extensive necrosis and macrophage infiltration seen by hematoxylin and eosin (Fig. 1).

The second analytical method used was temporal clustering using a data-scrubbing method, followed by statistical and temporal analyses by GeneSpring software. Data scrubbing was necessary due to non-expression or a low level (near background) of about one-third of the genes studied, as is typically seen in most Affymetrix profiling experiments in all organisms. Inclusion of the avg diff values for all "absent calls" leads to considerable artificial noise in temporal clustering, with random fluctuations at or below background hybridization levels showing "statistically significant" clustering with user- or candidate gene-defined patterns. We therefore required that each probe set show at least two "present calls" in the 12 expression profiles studied. This filtering was done using an SAS routine, where detection of two present calls leads to the inclusion of *all* avg diff values from all profiles for that probe set. A total of 6487 probe sets survived the selection by the SAS program, and then the absolute intensities for all 6487 probe sets for all profiles were input into the GeneSpring analytical package. A hierarchical clustering algorithm was then used to group probe sets based on shared expression patterns over the six time points (Fig. 2*B*). From this dendrogram, clusters of genes whose expression levels were up-regulated at the different stages of degeneration/regeneration are easily visualized (Fig. 2*B*). As expected, genes known to be involved in inflammation and immune response were up-regulated at early stages then down-regulated afterward. In contrast, expression of muscle-specific genes was down-regulated at early stages and then up-regulated at late stages (Fig. 2*B*).

Identification of Transcription Factor Targets by Temporal Clustering and Functional Assays—Further analysis of the profiles was restricted to MRF expression and, specifically, *MyoD*. The temporal patterns of expression of *Myf5*, *MyoD*, and *myogenin* were defined over the six degeneration/regeneration time points, with standard errors corresponding to duplicate profiles (Fig. 3*A*). Transcription levels were typically highly consistent between the two profiles for each time point, despite the fact that these were derived from independent muscles. All three MRFs showed up-regulation at 4 days following degeneration, consistent with formation of regenerating fibers at this time point (Figs. 1 and 3). *MyoD* transcription showed the expected biphasic pattern, with increases at both 12 h and 4 day post-injection.

We then looked at the temporal expression patterns of genes known to be targets of MyoD binding and transcriptional up-regulation (*AchRα*, *desmin*, and *Ulip*, Fig. 3*B*). Each showed a pattern consistent with up-regulation commensurate (4 day) or downstream (10 day) of MyoD.

The temporal resolution of the expression profiles obtained was relatively course, however, we felt it worthwhile to determine if candidate downstream targets of transcription factors could be defined by nucleating temporal clusters using a known downstream gene, *Ulip* (41) (Fig. 3*C*). We hypothesized that a subset of these nucleated clusters would be direct downstream targets of MyoD binding. This cluster does not contain all the known downstream targets of MyoD, because they do not exhibit the same expression pattern (Fig. 3*B*). This is probably due to regulation by factors other than MyoD in early (*e.g.* time 0) and late (*e.g.* day 10) stages. The genomic sequence databases of the murine and human genes corresponding to the *Ulip* clusters were searched for potential MyoD binding sites in their promoters (E-boxes); the promoters of 47 genes were

more than 2-fold by four pair-wised iterative comparison of duplicates at each injected time point to time 0. *Numbers* are indicated on the *top* of each *bar graph*. The number of differentially regulated genes continues increasing from 12 h to day 2 and then begins to decrease at day 4. *B*, hierarchical clustering of genes over a temporal series of muscle degeneration/regeneration expression profiles. Shown is the dendrogram derived from the temporal hierarchical clustering algorithm (GeneSpring). Each *row* represents a time point of the time series. Each *vertical colored bar* (*lower part* of figure) represents a single probe set (gene) in the profile (6487 total). *Vertical bars* in *red* indicate overexpression relative to the reference value, which is the median of the expression levels of the corresponding gene in all 12 profiles. *Blue* represents underexpression relative to the median. The *intensity* of each color represents the confidence of the data, which generally correlates with the -fold changes relative to the reference value. This algorithm clusters genes with similar expression patterns based on correlation coefficients. The distance between two genes on the dendrogram reflects the temporal expression profile similarity. Examples of three gene clusters representative of early macrophage infiltration (early up-regulated), muscle structural components (early down-regulated), and myogenic program transcription factors (late up-regulated) are shown *below* the dendrogram. *G-MCSFR*, granulocyte-macrophage colony-stimulating factor receptor; *PMM-SS2*, phosphoglycerate mutase muscle-specific subunit 2.

TABLE I

Cluster members showing potential MyoD binding sites (E-box; CAnnTG), and correlation with MyoD gel shift results

Underlined bases are E-boxes.

Gene Name	MyoD gel shift assay	Tested E-box sequence	Base pairs 5′ to transcription start site
Murine *Slug*	Yes	5′ TCTATTCACAGCTGTTCCAGA 3′	176bp
Human *Slug*	Yes	5′ TCTGTTCACAGCTGTCCCAGA 3′	262bp from ATG
Human *calpain 6*	Yes	5′ GATTCTGCACAGCTGTGTTAG 3′	614bp
Human *IGF1*	No	5′ GTTCCCCCAGCTGTTTCCTGTC 3′	94bp
Murine *Peg3*	No	5′ CTTCCAGCCATTTGCATTGTC 3′	565bp
	No	5′ GGTTGACCACATGCGATTCAG 3′	660bp
Human *Peg3*	No	5′ GGTTTTACATTTGAGCATCTC 3′	223bp
	No	5′ GACAGATGTGTACATTTGTCC 3′	252bp, 263bp
	No	5′ ATGTCTTTCATGTGTCCCAG 3′	360bp
Human *sFRP4*	No	5′ CGCGGCTGCAGCTGCCAAGGG 3′	113bp
Human *Slug*	No	5′ GAACCTCTCAGCTGTGATTGG 3′	224bp from ATG
Human *TM4SF6*	No	5′ CCCTTCTCAGTTGTGGACGCT 3′	41bp
	No	5′ GAAAGCTCCACTTGAAGACCT 3′	193bp
	No	5′ AAAGCACACAAGTGAGAAAAA 3′	532bp
	No	5′ CTTTCAACAAGTGGTGATTAT 3′	609bp
	No	5′ GGAAAAACCAGGTGGCTGGAA 3′	877bp
	No	5′ TCTGTAATCAGCTGGGTTTTG 3′	901bp

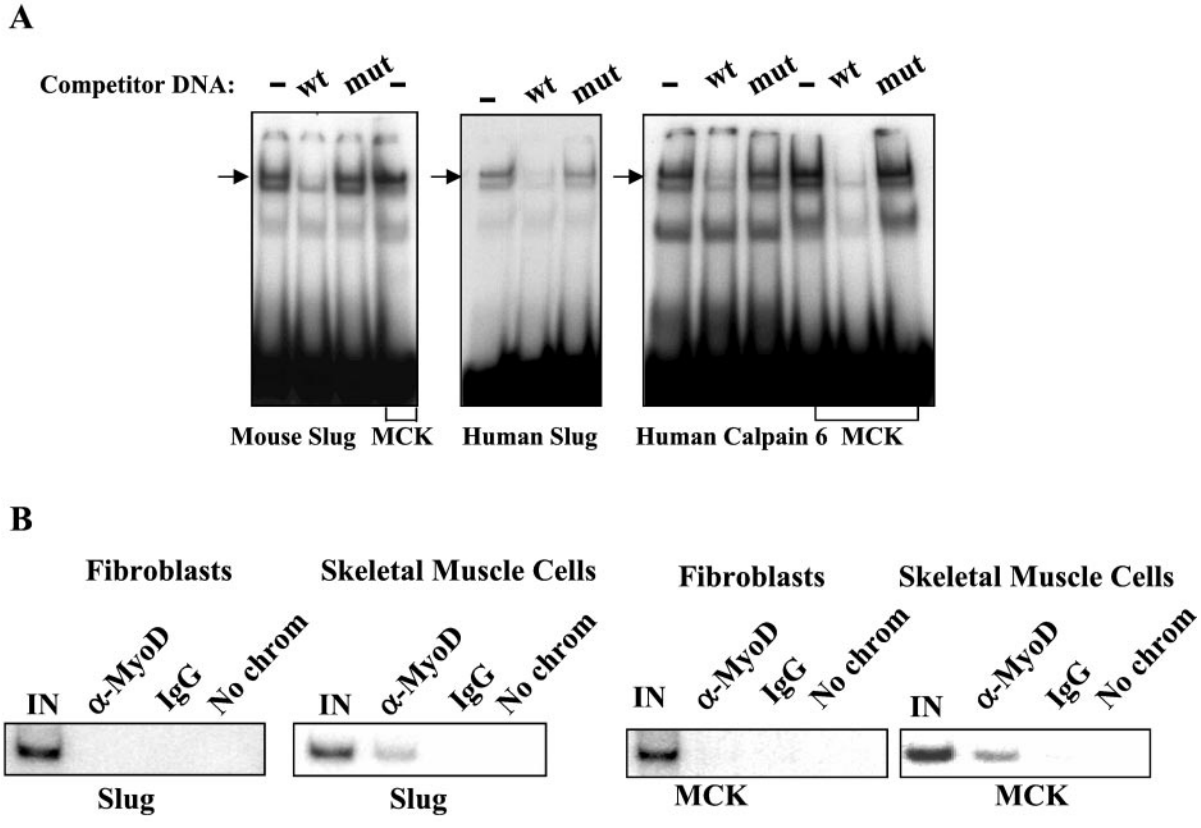

FIG. 4. **MyoD binds to the *Slug* putative promoter region *in vitro* and *in vivo*.** *A*, shown are gel shift assays with oligonucleotides corresponding to putative E-box MyoD consensus binding site sequences from the mouse *Slug* promoter, human *Slug* promoter, and human *calpain 6* promoter. Incubation of labeled oligonucleotides with C2C12 myonuclear extracts leads to band shift patterns that are indistinguishable from a known downstream target of MyoD, muscle creatine kinase (*MCK*). The presence of 100 times more unlabeled competitor DNA displaces the band shift, whereas mutant competitor DNA does not affect band shifting. These *in vitro* assays suggest *Slug* and *calpain 6* are potential MyoD downstream targets. *B*, shown are chromatin immunoprecipitation assays of *Slug* and *MCK* genes using a MyoD antibody. A 240-bp sequence located in the putative promoter region of *Slug* and a sequence in the *MCK* (positive control) promoter region were amplified in MyoD antibody-precipitated genomic DNA isolated from myotubes. Those sequences cannot be amplified from IgG immunoprecipitated DNA of myotube or MyoD antibody immunoprecipitated fibroblast DNA. These *in vivo* studies suggest that MyoD binds directly to the murine *Slug* promoter region in differentiated myotubes.

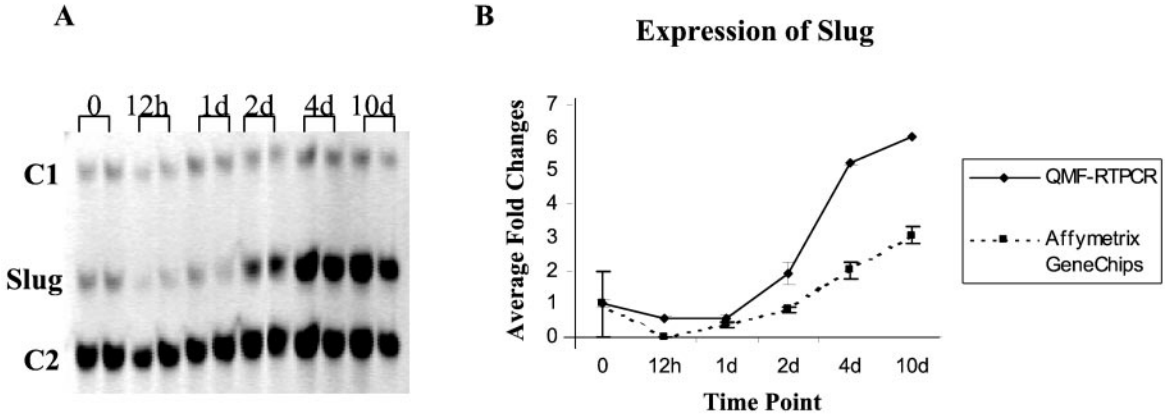

FIG. 5. **Confirmation of Slug expression by QMF-RT-PCR.** *A*, shown is the expression of Slug measured by 15-cycle multiplex fluorescent RT-PCR using infrared primers (QMF-RT-PCR). Two samples were tested at each time point. Expression of Slug dramatically increased at days 4 and 10 during muscle regeneration. NIPI-like protein (*C1*) and CMP-*N*-acetylneuraminic acid synthetase (*C2*) were used as controls. *B*, shown is the comparison of expression of Slug over the six-time point time course of muscle regeneration examined by QMF-RT-PCR and Affymetrix GeneChips. Expression levels of the duplicate samples of each time point were normalized to the average expression levels of controls. Normalized values thus represent -fold changes. QMF-PCR and Affymetrix results are consistent with each other. Both showed significant up-regulation of *Slug* at days 4 and 10 post-injection.

identified and studied. $GA_{nn}TG$ consensus within 1 kb upstream of the transcription start site were found in the mouse and/or human *Slug*, *calpain 6*, insulin-like growth factor 1 (*IGF1*), secreted frizzled-related protein 4 (*sFRP4*), paternally expressed gene *3* (*Peg3*), and transmembrane 4 superfamily member 6 (*TM4SF6*) genes (Table I).

To test whether MyoD was able to bind to these potential E-boxes, an *in vitro* gel shift assay was performed using myotube nuclear extracts and purified oligonucleotides corresponding to the E-box of each gene. A band shift identical to that of the positive control E-box from muscle creatine kinase (*MCK*) promoter was seen with mouse and human *Slug* oligonucleotides, and *calpain 6* (Fig. 4*A*). The DNA/protein complexes were competed by excess unlabeled wild-type *MCK* probes, but not excess unlabeled mutant *MCK* probes. The remaining candidate did not show a characteristic MyoD gel shift, and any labeled bands did not show appropriate competition patterns with control oligonucleotides, suggesting that these were not directly bound by MyoD (Table I). Interestingly, the potential MyoD binding sites in human *Slug*, murine *Slug*, and human *calpain 6* showed complete homology over a 9-bp sequence, including the E-box (CACAGCTGT; E-box consensus is underlined) (Table I).

MyoD Binds Slug in Vivo—To define if MyoD bound these potential novel downstream targets *in vivo*, we conducted chromatin immunoprecipitation (ChIP) assays using MyoD antibodies. We were not able to study *calpain 6* by this method, because only human promoter sequence was available, and the MyoD protein was not sufficiently expressed in human primary myogenic cells to carry out the assay (data not shown). In addition, *Slug* is thought to be an important mesodermal determination gene (42, 43), whereas the role of *calpain 6* is unknown. We therefore focused on the murine *Slug* gene for further experiments.

Chromatin immunoprecipitation experiments were carried out in MyoD-positive C2C12 murine myotubes. Mouse fibroblasts were employed as negative control, because they do not express MyoD. Endogenous DNA/protein complexes were cross-linked with formaldehyde and chromatin-sonicated, and MyoD-bound DNA fragments were immunoprecipitated with an anti-murine MyoD antibody. DNA cross-linked to MyoD was released by heating and tested for the presence of a known MyoD target (creatine kinase gene promoter) and the *Slug* promoter (Fig. 4*B*). From the genomic DNA fragments immunoprecipitated with MyoD antibody, a 240-bp region of the *Slug* promoter containing the MyoD binding site was amplified. No amplification was detected with IgG immunoprecipitates or using immunoprecipitated fibroblast chromatin (MyoD-negative cultures). This indicates that MyoD binds specifically to the Slug putative promoter region in myotubes.

Confirmation of Slug Expression in Muscle Regeneration by QMF-RT-PCR—We conducted quantitative multiplex fluorescence RT-PCR (QMF-PCR) to confirm the changes of the expression pattern of *Slug* over the six time points observed in the Affymetrix results (44). cDNA was synthesized from an equal amount of the total RNA of each sample. Infrared fluorescent-labeled PCR products were then amplified for 15 cycles from equal amount of cDNA and quantitated on automated sequencers. Expression of Slug was normalized to two control genes, NIPI-like protein and CMP-*N*-acetylneuraminic acid synthetase, both of which had shown no expression change (r = 0.99 with user-defined flat profile) across all profiles, and were at the same relative level (avg diff values) as *Slug* mRNA.

The -fold changes of *Slug* expression relative to time 0 were calculated for each time point. Expression of *Slug* was significantly up-regulated at day 4 and day 10 post-injection, which is consistent with that observed using Affymetrix GeneChip platform (Fig. 5).

Isolation and Functional Characterization of the Slug Promoter—Our *in vitro* binding and ChIP data indicated that MyoD was able to bind to a genomic, non-coding region of the *Slug* gene. To directly address whether the *Slug* promoter region employed in ChIP experiments contained *bona fide* regulatory regions, we subcloned it in two different reporter constructs. One if these constructs harbored the viral SV40 promoter-directing expression of the luciferase gene (SV40P-luc); the second contained the viral SV40 enhancer (SV40E-luc). The Slug genomic region was subcloned in both these constructs to generate the Slug-SV40P-luc and SV40E-Slug-luc reporters, respectively. The Slug-reporter constructs were transiently transfected into mouse fibroblasts, and luciferase activity was measured after 48 h. The results of these experiments indicate that indeed the *Slug* genomic region contains elements that support transcriptional activation. Furthermore, the experiments suggest that the Slug genomic region has the functional characteristics of a promoter (data not shown).

The Slug Promoter Is Activated during Muscle Differentiation and Is Directly Transactivated by MyoD—The results re-

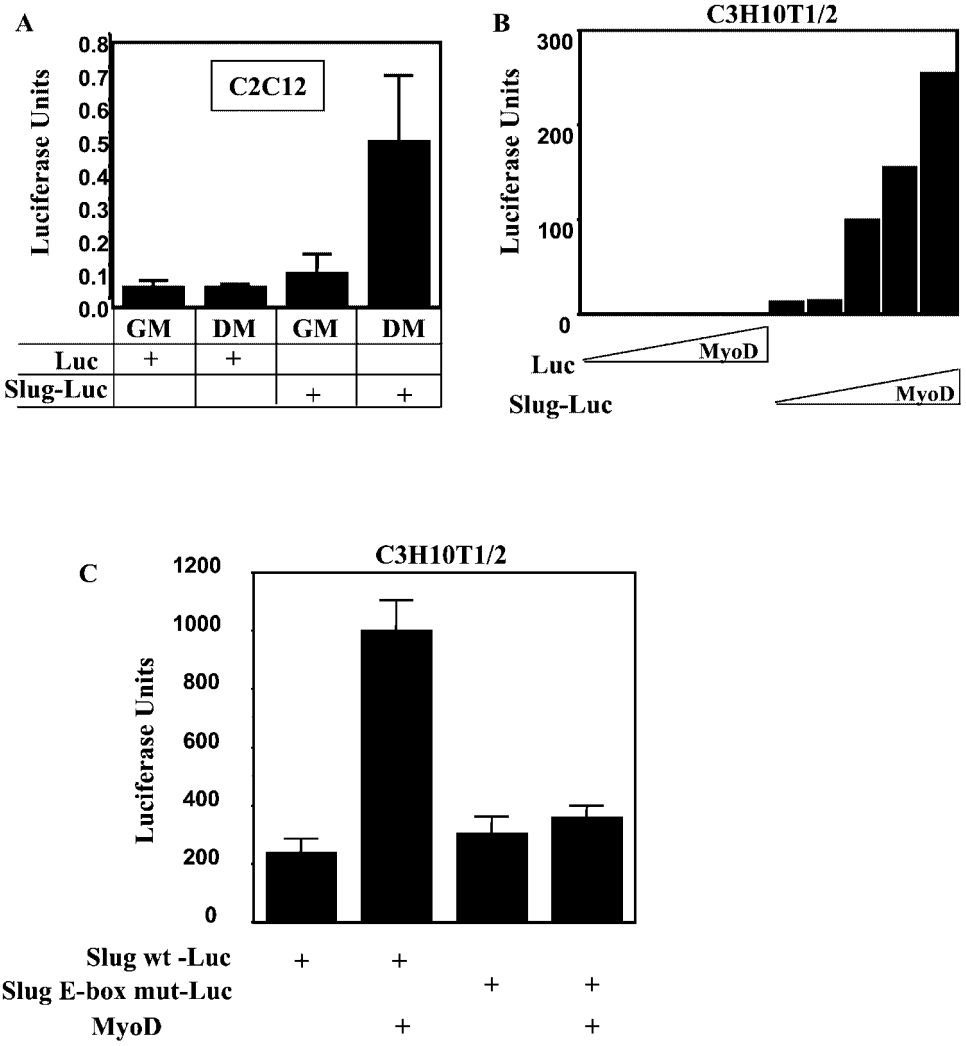

FIG. 6. **Reporter gene constructs with the putative *Slug* promoter MyoD binding site shows that the promoter element functions as a MyoD-sensitive positive regulatory element.** *A*, the *Slug* E-box acts as a positive promoter only in differentiated myogenic cells. Proliferating myoblast C2C12 cells (*GM*, growth medium) or differentiated myotubes (*DM*, differentiation medium) were transfected with 1 μg of the indicated reporter vectors and assayed for luciferase activity. *B*, the *Slug* promoter element is regulated by increasing MyoD levels. The indicated constructs (1 μg) were transfected into C3H10T1/2 mouse fibroblasts along with increasing concentrations of an *MyoD*-expressing plasmid (2, 5, 10, and 20 ng). After transfection, cells were cultured in differentiation medium to allow for MyoD activity. Luciferase assay was performed after 48 h. *C*, the E-box present in the *Slug* promoter is required for MyoD transactivation. C3H10T1/2 cells were transfected with either a *Slug* wild-type-luc or a *Slug* bearing a mutated E-box (*Slug-E-box mut-luc*) construct and a *MyoD* expression vector. After transfection, cells were cultured in differentiation medium to allow for MyoD activity. Luciferase assay was performed after 48 h.

ported in the preceding paragraph indicate that we had isolated a critical part of the *Slug* promoter. To more stringently show differentiation-specific regulation of *Slug* in response to MyoD levels, we subcloned the *Slug* MyoD binding sequence in a vector devoid of both promoter and enhancer elements to generate a Slug-luc reporter construct. The Slug-luc reporter construct was transfected in C2C12 skeletal muscle cells grown in conditions that either prevent (GM, growth medium) or favor (DM, differentiation medium) differentiation and transcriptional activity measured (Fig. 6*A*). It is well-established that MyoD is expressed in proliferating myoblasts, however, it is transcriptionally inactive at this stage because it is complexed to histone deacetylase 1 (22) and is incapable of interacting with its cognate DNA binding site. MyoD is again activated upon myoblast differentiation, and, as such, reporter activation was observed in differentiated myotubes, but not myoblasts, as expected for downstream targets of MyoD (Fig. 6*A*). The results of these experiments indicate that the *Slug* genomic region behaves as a promoter and that its transcriptional activation occurs in differentiated skeletal muscle cells.

Finally, we tested whether MyoD could transactivate the *Slug* promoter. The Slug-luc reporter was transfected in mouse fibroblasts in either the absence or presence of increasing concentration of a *MyoD* expression vector, and luciferase activity was measured. MyoD efficiently transactivated Slug-luc but did not activate the luciferase vector alone (Fig. 6*B*). To evaluate whether binding of MyoD to its cognate DNA binding site is necessary to activate transcription from the Slug promoter, we interrupted the integrity of the Slug E-box by introducing two single-point mutations and co-transfected the resulting mutated Slug-luc construct in mouse fibroblasts with a MyoD expression vector. Although the Slug-luc wild-type construct could be efficiently transactivated, the Slug-E-box mutant-luc remained transcriptionally inert, indicating that MyoD activates the Slug promoter by direct binding (Fig. 6*C*). These results show that the transcriptional activity of the Slug promoter is regulated during muscle differentiation and indicate that MyoD is one of the direct regulators of the *Slug* promoter.

Slug and Calpain 6 Are Up-regulated in Myoblast Differentiation—As a means of confirming the *in vivo* results, and to

investigate whether *Slug* and *calpain 6* expression were up-regulated during myoblast differentiation, we examined temporal expression profiling data of myoblast differentiation in cell culture. Expression of both *Slug* and *calpain 6* were increased at 24 h after myoblasts were switched to differentiation medium, corresponding to up-regulation of *MyoD* (Fig. 7). This indicates Slug and calpain 6 were up-regulated during early myoblast differentiation. Down-regulation of *Slug* at 48 h may be due to the presence of inhibitory factors expressed during the transition to myotubes in this cell line.

Slug−/− Mice Show Defects in Muscle Regeneration—The *Slug* gene and protein have been shown to modulate early mesoderm or neural ectoderm development in *Xenopus* and chick but have not been implicated in myogenic development or regeneration. To determine if the Slug protein played a role in muscle regeneration, we obtained *Slug* knock-out mice (45) and induced muscle regeneration by injection of CTX in both gastrocnemii of three animals. We then sacrificed the mice at 10 days after muscle regeneration.

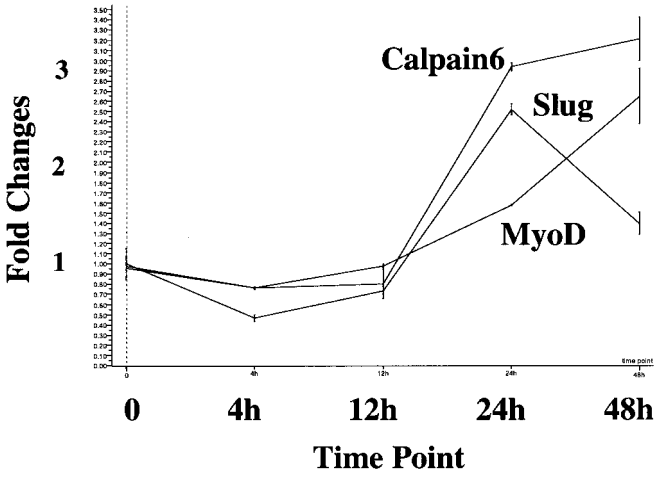

FIG. 7. **Slug and calpain 6 are up-regulated during myoblast differentiation in culture.** Shown is expression of *Slug*, *calpain 6*, and *MyoD* over five time points (0, 4, 12, 24, and 48 h) during C2C12 myoblast cell differentiation examined with the Affymetrix GeneChips U74Av2 platform. *Error bar* shows standard error derived from the duplicates at each time point. Expression of Slug and calpain 6 were increased at 24 h after cells were switched into differentiation medium, corresponding with up-regulation of MyoD, and expression of known MyoD targets, such as muscle creatine kinase.

Although the muscle of Slug null mice appeared histologically normal prior to CTX injection, it showed poor regeneration (Fig. 8, *A–D*). Regenerating muscle showed little evidence of successful formation of centrally nucleated regenerated myofibers, and the entire muscle group showed a diameter that was significantly smaller than normal regenerated murine muscle (Fig. 8*E*). We also tested for apoptosis in normal and *Slug* null regenerated muscle, because a single report in human lymphoblasts had suggested a role for Slug in inhibiting apoptosis. We did not see any evidence of increased apoptosis in regenerating *Slug−/−* muscle using antibodies against both caspase 3 and activated caspase 3 (data not shown). Taken together, these data are consistent with *Slug* being required for efficient regeneration of muscle.

DISCUSSION

Transcription Profiling to Define Transcriptional Cascades in Vivo—We presented a temporal series of expression profiles that define the cascade of gene expression changes during muscle regeneration *in vivo*. 10,000 genes were queried, with replicates for each of six time points from different mice. We used noise-filtering algorithms to limit further study to the 6,487 genes showing the most robust and reproducible data. We focused our analysis only on MyoD regulation and identification of novel downstream gene targets for the MyoD protein. However, all data is publicly available via our website (microarray.cnmcresearch.org) and the NCBI GEO data base and can be mined to study many additional questions.

The temporal profiles presented here are relatively course, with six time points over a range of 10 days of regeneration. This was sufficient to detect the expected temporal expression patterns of known myogenic regulatory factors (*MyoD*, *Myogenin*, and *Myf5*) and known downstream targets of MyoD (*AChRα*, *Ulip*, and *desmin*) (Fig. 3). Given the course nature of the temporal data, temporal clustering using known downstream targets might be expected to be sensitive but relatively nonspecific. Consistent with this hypothesis, query of the promoters of coordinately regulated genes clustering with known down-stream targets of MyoD showed a minority with potential E-box promoter elements ($CA_{nn}TG$) (Table I). Testing of 18 of these potential sites showed three promoters (murine *Slug*, human *Slug*, and human *calpain 6*) to show gel shifts consistent with known MyoD gel shifts (16%) (Fig. 4*A*). Interestingly, all three promoter elements, showing a gel shift consistent with MyoD binding, showed complete homology over a 9-bp se-

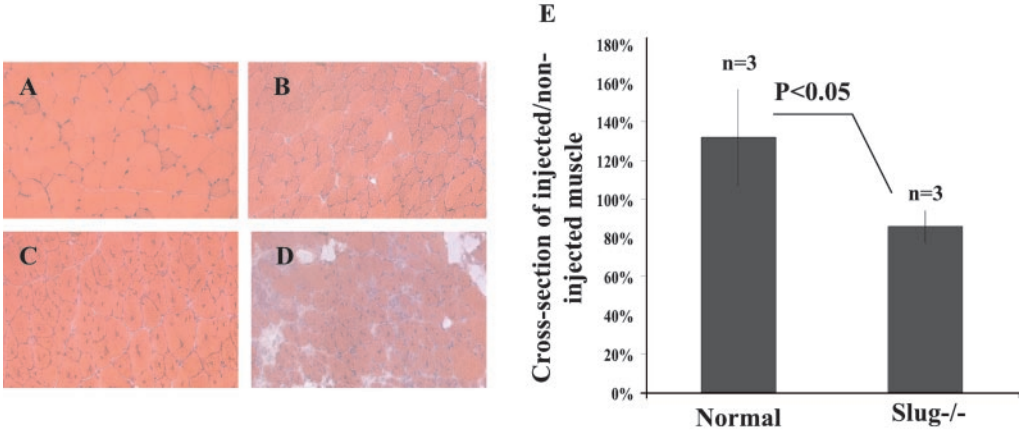

FIG. 8. **Slug knock-out mice are defective for muscle regeneration.** Normal and *Slug−/−* mouse gastrocnemii were induced to degenerate with CTX injection. Non-injected muscles (*A* and *B*) appear similar between normal mice (*B*) and *Slug* knock-outs (*B*). Examination of muscle histology 10 days following injection (*C* and *D*) shows normal muscle with successfully regenerated myofibers with central nuclei and well-defined myofiber architecture (*B*), whereas *Slug−/−* muscle shows poorly defined myotubes (*D*). Quantitation of cross sectional area of the gastrocnemii of normal and *Slug−/−* mice, before CTX injection and 10 days after regeneration, shows that *Slug−/−* exhibit poor regeneration (*E*). The area is expressed as a percentage change from non-injected.

quence, which was inclusive of the traditional E-box (CACAGCTGT). We confirmed co-expression of *MyoD*, *calpain 6*, and *Slug* in differentiating myogenic cells by studying expression in cultured C2C12 cells (Fig. 7). These data showed expression patterns consistent with *Slug* ad *calpain 6* being downstream of MyoD. The 24-h time point at which *calpain 6* and *Slug* were expressed corresponds to a stage of differentiating myocytes, prior to fusion to myotubes, where p21, myogenin, creatine kinase, and myosin heavy chain are all being transcriptionally activated.

We further characterized the murine *Slug* E-box promoter element, both to prove that this functioned as a positive promoter sequence and to confirm MyoD binding and regulation. We selected this promoter element for further study, because of the interest in *Slug* during development. Endogenous MyoD binding to the *Slug* promoter was shown by chromatin immunoprecipitation in myogenic cells (Fig. 4*B*), indicating that MyoD did indeed bind this element *in vivo*. To further test the nature of the novel E-box sequence, we tested a series of reporter constructs containing this element and showed that this sequence functioned as a promoter and not an enhancer, that transcriptional activity of this element was dependent on myogenic differentiation, and that the element was directly responsive to MyoD concentrations in transfected cells (Fig. 6). Thus, we have demonstrated that the *Slug* gene is a *bona fide* downstream target of MyoD.

Functional Significance of Slug in Muscle Regeneration—The temporal expression patterns of *Slug* and *calpain 6* were consistent with participation in muscle regeneration, and the finding of MyoD binding to their promoters is consistent with this hypothesis. We directly tested this hypothesis by studying the ability of *Slug* null muscle to regenerate following CTX injection. At 10 days post-injection, normal mouse gastrocnemii showed efficient formation of centrally nucleated myofibers, whereas *Slug* null mice evidenced poor regeneration with only relatively rare centrally nucleated regenerated fibers at this time point (Fig. 8). Measurement of the complete cross sectional area of the regenerating gastrocnemii showed a statistically significant decrease in muscle area, consistent with defective muscle regeneration in *Slug* null mice (Fig. 8*E*). These data suggest that the Slug protein is important for muscle regeneration, however, there are a number of possible developmental or molecular abnormalities that could give this result. Because Slug is a known transcription factor, *Slug* null mice may in fact show a failure of myogenic differentiation due to downstream consequences of loss of appropriate *Slug* expression. Alternatively, they could also show a paucity of myogenic precursor cells (satellite cells), have pre-existing defects of basal lamina or other scaffolding components, or any one, or have more of a plethora of defects unrelated to downstream targets of Slug binding.

In this context, it is relevant to discuss current knowledge concerning the normal function of Slug. Slug has been intensively studied (46) but has not previously been identified as being downstream of MyoD. Slug is a zinc finger protein of the Snail family. The *snail* locus was first identified through systematic screening of embryonic lethal phenotypes caused by mutation on the second chromosome of *Drosophila* (47). *Drosophila Snail* mutants fail to form ventral furrow in gastrulation and mesoderm (47, 48). The snail protein and its homologs in *Xenopus* (*Xsna*) and chicken (chicken *snail-like*), zebrafish (*snail1* and *snail2*), mouse (*Sna*), and human (*SNAI1*) contain four to six conserved zinc finger motifs at the carboxyl terminus and thus appear to be DNA-binding proteins, although their downstream targets are not yet clear.

Slug was identified as a subgroup of the snail family by screening a chick embryo cDNA library with a probe from *Xenopus* snail (42). Mouse *Slug* was expressed in migratory neural crest cells and mesoderm (43, 45, 49). Mice lacking the *Slug* gene show growth retardation and eye infections but do not show any overt abnormalities in mesoderm formation or neural crest cell generation and migration (45). This is despite the fact that *Slug* is likely to play regulatory roles in multiple processes, because it is expressed in developing limb bud, cartilage, kidney, lung, and many mouse and human adult tissues, including skeletal muscle (49, 50). Our results indicate that the role of *Slug* in skeletal myogenesis could be uncovered only after inducing muscle regeneration. A recent study indicated that *Xenopus Slug* promoter was regulated by Lef/β-catenin complex, a component of the *Wnt* signaling pathway (51), and the *Wnt* pathway has recently been found to be critical for early muscle development (1, 52, 53).

MyoD null mice are born with intact muscle, but show significantly delayed muscle regeneration (27). We hypothesize that *MyoD* null mice may be unable to appropriately express *Slug* and that a component of the abnormal regeneration of *MyoD* null mice is shared with the abnormal regeneration we have observed here in *Slug* null mice. However, distinguishing between the many possible defects in transgenic knock-out mice will require considerable further study.

Our data demonstrate that expression profiling of vertebrate tissues *in vivo* appears to have the requisite sensitivity to detect the complex interplay of transcription factors and downstream target genes in response to specific stimuli. Importantly, the transcription profiles presented here are publicly available (microarray.cnmcresearch.org/pga), and any transcription factor or defined downstream target can be used to nucleate temporal clusters and define potential novel downstream targets, as we have shown here for MyoD.

REFERENCES

1. Cossu, G., and Borello, U. (1999) *EMBO J.* **18,** 6867–6872
2. Dhoot, G. K., Gustafsson, M. K., Ai, X., Sun, W., Standiford, D. M., and Emerson, C. P., Jr. (2001) *Science* **293,** 1663–1666
3. Coutelle, O., Blagden, C. S., Hampson, R., Halai, C., Rigby, P. W., and Hughes, S. M. (2001) *Dev. Biol.* **236,** 136–150
4. Davis, R. L., Weintraub, H., and Lassar, A. B. (1987) *Cell* **51,** 987–1000
5. Wright, W. E., Sassoon, D. A., and Lin, V. K. (1989) *Cell* **56,** 607–617
6. Edmondson, D. G., and Olson, E. N. (1989) *Genes Dev.* **3,** 628–640
7. Braun, T., Buschhausen-Denker, G., Bober, E., Tannich, E., and Arnold, H. H. (1989) *EMBO J.* **8,** 701–709
8. Puri, P. L., and Sartorelli, V. (2000) *J. Cell. Physiol.* **185,** 155–173
9. Weintraub, H., Davis, R., Lockshon, D., and Lassar, A. (1990) *Proc. Natl. Acad. Sci. U. S. A.* **87,** 5623–5627
10. Wentworth, B. M., Donoghue, M., Engert, J. C., Berglund, E. B., and Rosenthal, N. (1991) *Proc. Natl. Acad. Sci. U. S. A.* **88,** 1242–1246
11. Van de Klundert, F. A. J. M., Jansen, H. J., and Bloemendal, H. (1994) *J. Biol. Chem.* **269,** 220–225
12. Marshall, P., Chartrand, N., and Worton, R. G. (2001) *J. Biol. Chem.* **276,** 20719–20726
13. Buskin, J. N., and Hauschka, S. D. (1989) *Mol. Cell. Biol.* **9,** 2627–2640
14. Rudnicki, M. A., and Jaenisch, R. (1995) *Bioessays* **17,** 203–209
15. de la Serna, I. L., Carlson, K. A., and Imbalzano, A. N. (2000) *Nat. Genet.* **27,** 187–190
16. Sartorelli, V., Puri, P. L., Hamamori, Y., Ogryzko, V., Chung, G., Nakatani, Y., Wang, J. Y., and Kedes, L. (1999) *Mol. Cell* **4,** 725–734
17. McKinsey, T. A., Zhang, C. L., Lu, J., and Olson, E. N. (2000) *Nature* **408,** 106–111
18. Steinbac, O. C., Wolffe, A. P., and Rupp R. A. (2000) *Biol. Chem.* **381,** 1013–1016
19. Mal, A., Sturniolo, M., Schiltz, R. L., Ghosh, M. K., and Harter, M. L. (2001) *EMBO J.* **20,** 1739–1753
20. McKinsey, T. A., Zhang, C. L., and Olson, E. N. (2001) *Curr. Opin. Genet. Dev.* **11,** 497–504
21. Polesskaya, A., and Harel-Bellan, A. (2001) *J. Biol. Chem.* **276,** 44502–44503
22. Puri, P. L., Iezzi, S., Stiegler, P., Chen, T. T., Schiltz, R. L., Muscat, G. E., Giordano, A., Kedes, L., Wang, J. Y., and Sartorelli, V. (2001) *Mol. Cell* **8,** 885–897
23. Perry, R. L., Parker, M. H., and Rudnicki, M. A. (2001) *Mol. Cell* **8,** 291–301
24. Blackwell, T. K., and Weintraub, H. (1990) *Science* **250,** 1104–1110
25. Liu, S., Spinner, D. S., Schmidt, M. M., Danielsson, J. A., Wang, S., and Schmidt, J. (2000) *J. Biol. Chem.* **275,** 41365–41368
26. Becker, J. R., Dorman, C. M., McClafferty, T. M., and Johnson, S. E. (2001) *Exp. Cell Res.* **267,** 135–143
27. Rudnicki, M. A., Braun, T., Hinuma, S., and Jaenisch, R. (1992) *Cell* **71,** 383–390

28. Megeney, L. A., Kablar, B., Garrett, K., Anderson, J. E., and Rudnicki, M. A. (1996) *Genes Dev.* **10,** 1173–1183
29. Yablonka-Reuveni, Z., Rudnicki, M. A., Rivera, A. J., Primig, M., Anderson, J. E., and Natanson, P. (1999) *Dev. Biol.* **210,** 440–455
30. Montarras, D., Lindon, C., Pinset, C., and Domeyne, P. (2000) *Biol. Cell* **92,** 565–572
31. Cornelison, D. D., Olwin, B. B., Rudnicki, M. A., and Wold, B. J. (2000) *Dev. Biol.* **224,** 122–137
32. White, J. D., Scaffidi, A., Davies, M., McGeachie, J., Rudnicki, M. A., and Grounds, M. D. (2000) *J. Histochem. Cytochem.* **48,** 1531–1544
33. Chen, J. C., Love, C. M., and Goldhamer, D. J. (2001) *Dev. Dyn.* **221,** 274–288
34. Cooper, R. N., Tajbakhas, S., Mouly, V., Cossu, G., Buckingham, M., and Butler-Browne, G. S. (1999) *J. Cell Sci.* **112,** 2895–2901
35. Launay, T., Armand, A. S., Charbonnier, F., Mira, J. C., Donsez, E., Gallien, C. L., and Chanoine, C. (2001) *J. Histochem. Cytochem.* **49,** 887–899
36. Eisen, M. B., Spellman, P. T., Brown, P. O., and Botstein, D. (1999) *Proc. Natl. Acad. Sci. U. S. A.* **95,** 14863–14868
37. Tavazoie, S., Hughes, J. D., Campbell, M. J., Cho, R. J., and Church, G. M. (1998) *Nat. Genet.* **22,** 281–285
38. Chen, Y.-W., Zhao, P., Boroup, R., and Hoffman, E. P. (2000) *J. Cell Biol.* **151,** 1321–1336
39. Boyd, K. E., Wells, J., Gutman, J., Bartley, S. M., and Farnham, P. J. (1998) *Proc. Natl. Acad. Sci. U. S. A.* **95,** 13887–13892
40. Bakay, M., Chen, Y.-W., Borup, R., Zhao, P., Nagaraju, K., and Hoffman, E. (2002) *BMC Bioinformatics* **3,** 4
41. Matsuo, T., Stauffer, J. K., Walker, R. L., Meltzer, P., and Thiele, C. J. (2000) *J. Biol. Chem.* **275,** 16560–16568
42. Nieto, M. A., Sargen, M. G., Wilkinson, D. G., and Cooke, J. (1994) *Science* **264,** 835–839
43. Savagner, P., Yamada, K. M., and Thiery, J. P. (1997) *J. Cell Biol.* **137,** 1403–1419
44. Zhou, J. H., and Hoffman, E. P. (1994) *J. Biol. Chem.* **269,** 18563–18571
45. Jiang, R., Lan, Y., Norton, C. R., Sundberg, J. P., and Gridley, T. (1998) *Dev. Biol.* **198,** 277–285
46. Hemavathy, K., Ashraf, S. I., and Ip, Y. T. (2000) *Gene* **257,** 1–12
47. Nusslein-Volhard, C., Wieschaus, E., and Kluding, H. (1984) *Wilhelm Roux's Arch. Dev. Biol.* **193,** 267–282
48. Grau, Y., Carteret, C., and Simpson, P. (1984) *Genetics* **108,** 347–360
49. Sefton, M., Sanchez, S., and Nieto, M. A. (1998) *Development* **125,** 3111–3121
50. Cohen, M. E., Yin, M., Paznekas, W. A., Schertzer, M., Wood, S., and Jabs, E. W. (1998) *Genomics* **51,** 468–471
51. Vallin, J., Thure, R., Giacomello, E., Faraldo, M. M., Thiery, J. P., and Broders, F. (2001) *J. Biol. Chem.* **276,** 30350–30358
52. Hirsinger, E., Duprez, D., Jouve, C., Malapert, P., Cooke, J., and Pourquie, O. (1997) *Development* **124,** 4605–4614
53. Ridgeway, A. G., Petropoulos, H., Wilton, S., and Skerjanc, I. S. (2000) *J. Biol. Chem.* **275,** 32398–32405